Anomalous Ionization in the MPD Thruster*

Edgar Y. Choueiri
Electric Propulsion and Plasma Dynamics Laboratory
Princeton University, Princeton, NJ 08544, USA

Hideo Okuda
Princeton Plasma Physics Laboratory
Princeton University, Princeton, NJ 08544, USA

Abstract

We present a prescription for the electron energy distribution function that allows the representation of suprathermal electron tails such as those produced by the nonlinear effects of plasma microturbulence. The model is specified by a bulk temperature, a tail fraction, a tail energy scaling parameter and a tail spread parameter. The parametric distribution function is combined with a multi-level atomic model of argon and used to calculate the reaction rates for 23 collisional excitation transitions from ground state by electron impact by applying a high-accuracy quadrature on the convolution integrands containing the appropriate cross-sections. The prime goal was the study of the parametric dependencies of the minimum ionization characteristic length on the tail parameters. Calculations are compared with the recent measurements of the dimensions of an ionization "front" observed in a low-power MPD thruster by Randolph et. al. The ionization length which is at least 10 times smaller than that calculated assuming Maxwellian statistics is shown to be more consistent with distributions having suprathermal tail fractions and energies that could be produced by plasma microturbulence. Tail fractions of about 1%, under some conditions, can reduce the spatial extent of ionization to the millimeter level. Typical tail parameters obtained from a particle simulation code designed for the study of anomalous ionization were used to illustrate the model's implications.

*This work is supported by a grant from the Air Force Office of Scientific Research (AFOSR Grant No. F49620-93-1-0222) and the National Aeronautics and Space Administration under contract NASA-954997.

1 Introduction

Ionization represents a largely irrecoverable energy sink in magnetoplasmadynamic (MPD) thrusters. This is mostly due to the fact that, for typical temperatures and pressures of most plasma thrusters, the plasma flow through the chamber is essentially "frozen" with respect to recombination[1] (i.e. the plasma residence time scale is much shorter than the recombination characteristic time). While anode region losses dominate at low power levels, at higher power (above 100 kW) ionization losses become more dominant, as a fraction of the thrust inefficiency, for many propellants and under nominal operation.

Until recently, there has been only *indirect* evidence that the ionization might be related to collective effects (i.e. oscillations and turbulence in the plasma). Early speculations[2] (1985) were motivated by the importance of the critical ionization velocity (CIV) ($v_{ci} \equiv (2\epsilon_i/M)^{1/2}$ where ϵ_i and M are the ionization potential and atomic mass) as a scaling parameter and its ability to reduce measured voltage or thrust curves of self-filed thrusters to one curve largely independent of mass flow rate or propellant for many monatomic gases[3]. Scaling with v_{ci} is characteristic of many situations in plasma dynamics[4] where collective effects are present. In CIV situations, plasma instabilities extract available kinetic energy from the flow and use it produce suprathermal electrons that can substantially enhance ionization thus tying the directed flow energy to the ionization sink. In the case of the MPD thruster plasma, such a tie can exist through the effects of current driven instabilities which rely on the current which is, in turn, responsible for the production of the electromagnetic body force that is driving the flow. The presence of such plasma instabilities in the MPDT plasma, has

been established through recent theoretical and experimental studies[5, 6, 7].

The earliest experimental evidence of anomalous ionization (1968) comes from a spectroscopic study by Abramov et .al. that was briefly reported in [8]. In that study, a thin ionization front was observed upstream in the chamber and had a thickness much smaller than the classical ionization length. In the same study, anomalously high level of radiation was also measured and could not be accounted for on the basis of a 2 eV Maxwellian electron distribution. The authors invoked collective phenomena as responsible for these effects.

Most recently, (1992) Randolph et. al. reported the results of a detailed spectroscopic study of ionization[9]. In that study, the ionization front was observed and its thickness measured at a few millimeters. A model for collisional excitation of argon was used to calculate the smallest ionization length that can be accounted for on the basis of a Maxwellian distribution and was found to be between 1 and 3 orders of magnitude larger than the measured value.

Ionization in the MPD thruster has been the focus of a number of theoretical and numerical studies[10, 11, 12]. The emphasis was on either the non-equilibrium aspects of ionization or its role in ignition. There has been no attempt, to date, to address the impact of non-Maxwellian distributions, such as those produced by collective effects, on ionization.

This paper aims at a first contribution in this direction. We start in Section 2, with a model for the electron energy distribution function that allows the representation of suprathermal electron tails such as those produced by the nonlinear effects of plasma microturbulence. In Section 3, we describe aspects of the calculations of collisional excitation reaction rates that are central to our investigation. The resulting numerical model is then used in Section 4 for a study of the parametric dependencies of the minimum ionization characteristic length on the tail parameters. Calculations are compared with the recent measurements of the dimensions of the ionization "front" observed in a low power MPD thruster by Randolph et. al.[9]. Finally, is Section 5, typical tail parameters obtained from a particle simulation code designed for the study of anomalous ionization are used as an example.

2 Electron Distribution Function with a Suprathermal Tail

We start by assuming that the bulk of the electrons corresponding to a fraction $(1-\mu)$ of the entire distribution (where μ is the tail fraction), are represented by a Maxwellian with a temperature T_B

$$\left(\frac{dN}{N}\right)_B = \frac{4v^2}{\pi^{1/2}(2kT_B/m)^{3/2}} \exp\left[-mv^2/2kT_B\right] dv, \tag{1}$$

where all symbols are standard and the B subscripts refer to the "bulk" part of the distribution.

In order to control the extent and shape of the tail, we introduce a distribution for the fraction μ representing the suprathermal tail contribution, with a velocity drift u_0 and its own equivalent "temperature" T_T which we will refer to as the "tail energy scaling parameter",

$$\left(\frac{dN}{N}\right)_T = \frac{\frac{4v^2}{\pi^{1/2}(2kT_T/m)^{3/2}} \exp\left[-m(v-u_0)^2/2kT_T\right]}{\Omega} dv. \tag{2}$$

where the T subscripts refer to the "bulk" part of the distribution and Ω is a normalization term that must be such that

$$\int_0^\infty \left(\frac{dN}{N}\right)_T = 1. \tag{3}$$

Ω is therefore

$$\begin{aligned} \Omega &= \int_0^\infty \frac{4v^2}{\pi^{1/2}\left(\frac{2kT_T}{m}\right)^{3/2}} \exp\left[-\frac{m(v-u_0)^2}{2kT_T}\right] dv \\ &= 2 + \left(2\frac{u_d}{v_{tT}}\right)^2 \end{aligned} \tag{4}$$

where $v_t = (2kT/m)^{1/2}$ is the thermal velocity.

The composite distribution function $f(v)$ is the sum of the bulk Maxwellian and the tail model adjusted by their respective fractions,

$$f(v)dv = (1-\mu)\left(\frac{dN}{N}\right)_B + \mu\left(\frac{dN}{N}\right)_T \tag{5}$$

A parametric plot showing the shape of the resulting distribution and its tail is shown in Fig. (1) where a bulk 2 eV temperature (8.4×10^5 m/s) was chosen along with a tail energy scaling parameter of 6.4 eV (for relevance to the calculations in the following sections). The drift speed was set equal to the thermal

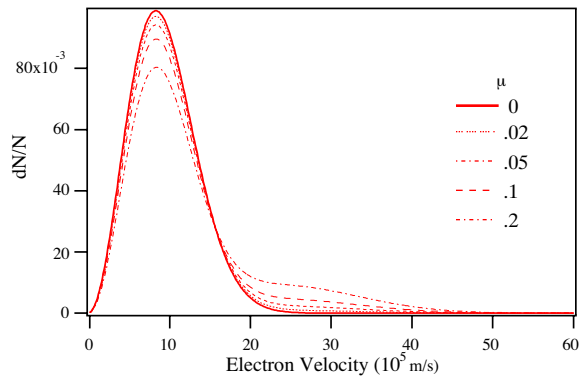

Figure 1: Adopted distribution model for a range of tail fractions, μ. T_t=6.4, $u_d = v_{tT} = 15 \times 10^5$ m/s.

velocity at that "temperature" i.e. 15×10^5 m/s and the tail fraction was varied parametrically.

The integral of $f(v)$ is plotted as a function of v in Fig. (2) showing the contribution to the integral of a given velocity range with the varying tail fraction, μ.

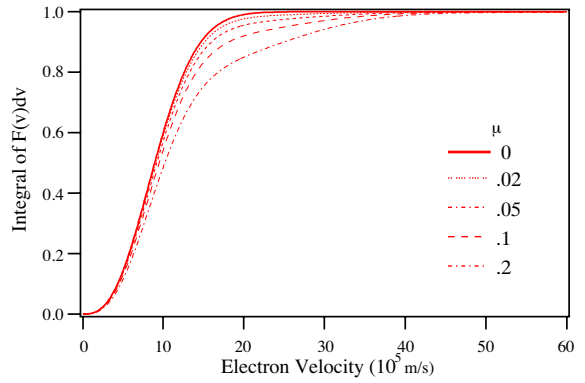

Figure 2: Integral of the adopted distribution model for a range of tail fractions, μ. T_t=6.4, $u_d = v_{tT} = 15 \times 10^5$ m/s.

Since our goal is the calculation of reaction rates which are obtained by weighing the cross sections with $vf(v)$ and integrating from a certain reaction energy level to infinity, we choose to use the following convenient parameters.

$$u_{ij} \equiv \frac{\epsilon_{ij}}{kT}; \qquad U_{ij} \equiv \frac{\epsilon}{\epsilon_{ij}}; \tag{6}$$

where the energy ϵ becomes the implicit variable and ϵ_{ij} represents the energy involved in going from level i to level j. The resulting model for the distribution function becomes

$$\begin{aligned} f(U_{ij})dU_{ij} = (1-\mu)\frac{2}{\pi^{1/2}} u_{ij}^{3/2} U_{ij}^{1/2} \times \\ \exp\left[-u_{ij}U_{ij}\right] dU_{ij} \\ +\mu \frac{e^{-\tau^2}}{\pi^{1/2}\left(1+2\tau^2\right)} u_{ij}^{3/2} U_{ij}^{1/2} \times \\ \exp\left[-u_{ij}U_{ij} + 2\tau u_{ij}^{1/2} U^{1/2}\right] dU_{ij} \end{aligned} \tag{7}$$

where we have also introduced the tail spread parameter τ defined by

$$\tau \equiv \frac{u_d}{v_{tT}}. \tag{8}$$

3 Reaction Rate Models for Collisional Excitation

Randolph et. al.[9] treated the case of a Maxwellian distribution and calculated a most conservative estimate of the ionization length, λ_i, (i.e. much shorter than would be predicted by a more accurate model). They found that even the most conservative estimate is still more than an order of magnitude longer than their experimental measurements. For the sake of continuity we follow their conservative assumptions. Namely, we neglect all reactions that tend to increase λ_i and thus limit ourselves to collisional excitation and neglect the reverse processes. This also carries the implicit assumption that once an atom is in a highly excited state it is easily (and thus is considered) ionized. Radiative absorption is one mechanism that could possibly enhance ionization and thus shorten λ_i but it was not considered in ref. [9] with the argument that it should not be substantial at the low density conditions of the low power MPD thrusters[13].

In essence such estimates represent the lowest bound on λ_i for a given set of conditions.

In order to estimate the impact of distributions with suprathermal tails on shortening the effective ionization length from its classical values, we need to use the above model along with the relevant cross-sections to calculate the associated reaction rates.

The reaction rates R_{ij} we are seeking are obtained from

$$R_{ij} = \langle \sigma_{ij} v \rangle = \int_1^\infty v_{th} u_{ij}^{1/2} U_{ij}^{1/2} \sigma_{ij} f\left(U_{ij}\right) dU_{ij} \tag{9}$$

Level n	Designation	Excitation energy (eV)	Type of transition	Coefficients α_{1j}^F or $\alpha_{1j}^A f_{1j}^A, \beta_{1j}$
1	$3p^6$	0	-	-
2	$4s[3/2]_2$	11.548	S	6.70×10^{-2}
3	$4s[3/2]_1$	11.624	A	1.92×10^{-2},4
4	$4s'[1/2]_0$	11.723	S	9.50×10^{-3}
5	$4s'[1/2]_1$	11.828	A	4.62×10^{-2},4
6	$4P[1/2]_1$	12.907	P	3.5×10^{-2}
7	$4P[3/2]_{1,2}, [5/2]_{2,3}$	13.116	P	1.15×10^{-1}
8	$4P'[3/2]_{1,2}$	13.295	P	3.50×10^{-2}
9	$4P'[1/2]_1$	13.328	P	7.00×10^{-3}
10	$4P[1/2]_0$	13.273	P	7.00×10^{-3}
11	$4P'[1/2]_0$	13.480	P	3.50×10^{-2}
12	$3d[1/2]_{0,1}, [3/2]_2$	13.884	S	1.50×10^{-1}
13	$3d[7/2]_{3,4}$	13.994	S	9.00×10^{-2}
14	$3d'[3/2]_2, [5/2]_{2,3}$	14.229	P	4.20×10^{-2}
15	$5s'$	14.252	A	3.71×10^{-3},4
16	$3d[3/2]_1, [5/2]_{2,3} + 5s$	14.090	A	3.33×10^{-2},4
17	$3d'[3/2]_1$	14.304	A	1.79×10^{-2},2
18	$5p$	14.509	P	7.00×10^{-2}
19	$5p'$	14.690	P	5.00×10^{-2}
20	$4d + 6s$	14.792	A	5.15×10^{-2},1
21	$4d' + 6s'$	14.976	A	3.06×10^{-2},1
26	$5d' + 7s'$	15.324	A	6.50×10^{-4},1
27	$5d + 7s$	15.153	A	3.69×10^{-2},1
33	$6d + 8s$	15.347	A	2.40×10^{-2},1

Table 1: Data for the 23 transitions considered in our calculations. A, optically allowed; P, parity-forbidden; S, spin-forbidden transitions. From ref. [15]

where σ_{ij} is the cross-section for the transition in question. Since we are dealing with excitation by electron impact from the ground state, we have $i = 1$.

For cross-sections of atomic excitation by electron-impact, we use the well-established semi-empirical formulae of Drawin[14]:

For allowed transitions the cross-section σ_{ij}^A is:

$$\sigma_{ij}^A = 4\pi a_0^2 \left(\frac{\epsilon_1^H}{\epsilon_{ij}}\right)^2 f_{ij}^A \alpha_{ij}^A \left[\frac{U_{ij}-1}{U_{ij}^2}\right] \ln\left(1.25\beta_{ij}U_{ij}\right). \tag{10}$$

For parity-forbidden transitions the cross-section σ_{ij}^P is:

$$\sigma_{ij}^P = 4\pi a_0^2 \alpha_{ij}^P \left[\frac{U_{ij}-1}{U_{ij}^2}\right]. \tag{11}$$

For spin-forbidden transitions the cross-section σ_{ij}^S is:

$$\sigma_{ij}^S = 4\pi a_0^2 \alpha_{ij}^S \left[\frac{U_{ij}^2-1}{U_{ij}^5}\right]. \tag{12}$$

In the above, f_{ij}^A is the absorption oscillator strength for optically allowed transitions, α_{ij} and β_{ij} are fit coefficients. All these parameters are part of the atomic physics model adopted for the calculations (see Table 3). Finally, ϵ_1^H is the ionization potential of hydrogen from ground state.

We consider 23 known excitation transitions from the ground level of the argon atom. These levels are part of the 65-level lumped atomic model for argon compiled and described by Vlček in ref. [15]. All the information needed to represent these 23 transitions in the above equations are listed in Table 3 extracted from ref. [15].

4 Results

The integral in Eq. (9) is evaluated with a 16-point Gauss-Legendre quadrature to insure high accuracy.

In order to keep continuity with the previous work, we use the expression for λ_i used by Randolph et. al[9]

$$\lambda_i \simeq \frac{v_f}{n_e \Sigma_{j>1} R_{1j}} \tag{13}$$

where v_f is the flow velocity and n_e is the electron density. In order to find the shortest predicted λ_i we set v_f to its lowest value in the MPD thruster $v_f = v_{\text{inlet}} \simeq 320\ m/s$ and set n_e to the highest possible density for the low power MPDT ($n_e = 1 \times 10^{14}$ cm^{-3}). In the same spirit we choose for the electron (bulk) temperature T_B the high end of the values measured for the low power thruster (i.e. T_B=2 eV). We set the tail spread parameter τ to unity (i.e. $u_d = v_{tT}$) to reduce the number of tail control parameters and vary the other two tail quantities: the tail fraction, μ and the tail energy scaling parameter T_T.

Figure (3) shows results from these calculations along with the experimental bounds . The Maxwellian limit is obtained when the tail fraction goes to zero. We recover there the result of ref. [9]. It is thus clear that even under the most favorable conditions, Maxwellian electrons cannot account for the smallness of λ_i. It is also clear that at these conditions, tail fractions of the order of a few percent can bring down λ_i in the millimeter range that contains the experimentally measured values.

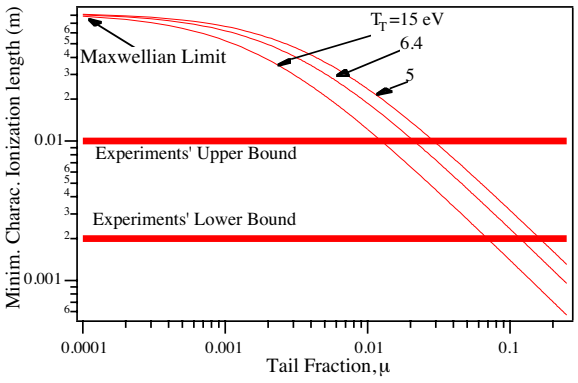

Figure 3: Calculated minimum values of λ_i as a function of the tail fraction. T_e=2.0 eV, $\tau = 1$. Experimental values from ref. [9]

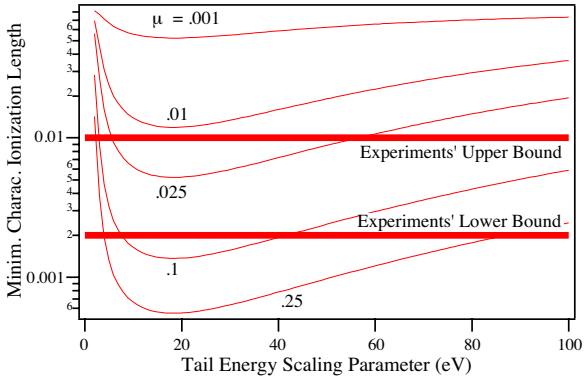

Figure 4: Calculated minimum values of λ_i as a function of the tail energy scaling parameter, T_T. T_e=2.0 eV, $\tau = 1$. Experimental values from ref. [9]

It should also be noted that λ_i is not always a monotonic function of the tail parameters due to the complex interplay between the tail's shape and the cross-section-energy dependence. Depending on the energy level and the tail parameters, contributions to λ_i from allowed, spin-forbidden and parity-forbidden transitions alternate in importance.

An illustration of how increasing the tail's energy scaling parameter T_T can either increase or decrease λ_i is shown in Fig. (4). The curves go through a minimum around 20 eV. At that minimum, tail fractions of 1 percent and higher can bring λ_i down to within the experimental bounds.

5 Insight from Particle Simulations

The calculations above are based on assumed or parametrically varied tail parameters. Some a priori knowledge of the extent of the departure of the distribution function from the Maxwellian case is required and can be in principle be obtained from 1) Experiments, 2) nonlinear or quasilinear plasma theory or 3) particle simulations.

In this section we briefly illustrate how some insight on the sizing of suprathermal tail parameters can be obtained from particle simulation codes.

In particular, we use a particle code that we have been applying to the study of anomalous ionization through CIV tests using gas releases from an orbiting spacecraft. The code is a $2\frac{1}{2}$-dimensional, electro-

static particle-in-cell (PIC) code in a slab geometry. It includes guiding center approximations for the electrons and the full dynamics for the ions and allows simulations with real mass ratios. A Monte Carlo collision operator is added to the self-consistent particle motion in order to model various collisional processes inherent to interaction studies. The code's nucleus has been described in detail by Lee and Okuda[16].

We have been studying, using this code, the CIV test conducted recently onboard the ATLAS-1 mission[17]. The simulation geometry is shown schematically in Fig. (5).

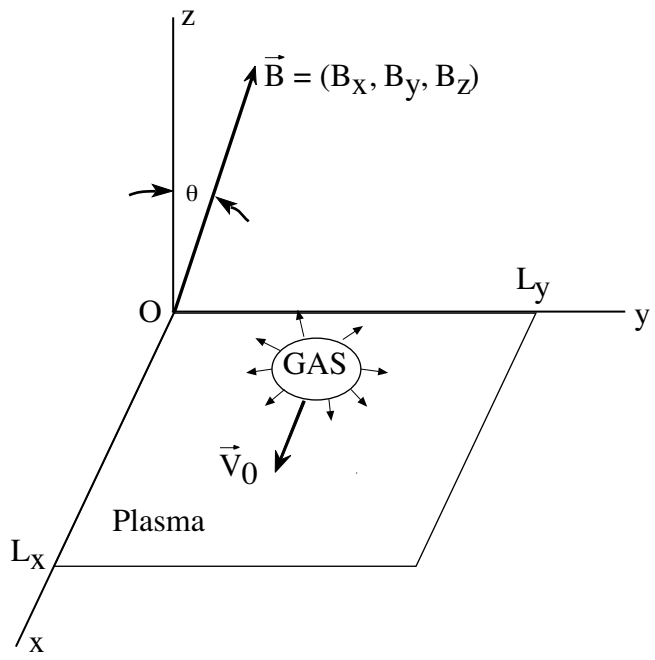

Figure 5: Configuration for the particle simulation study of anomalous ionization. The neutral gas (xenon) which is injected from an orbiting spacecraft is expanding and moving with respect to the ionospheric plasma with the orbital velocity v_0 and is subject to collective ionization (CIV).

The dimensions of the simulations are 256 by 1024 cm and the plasma conditions are those of the ionosphere in LEO at high latitudes. In particular, we have $n_e = 2 \times 10^5 \text{cm}^{-3}$, $T_e = 0.1\ eV$ and the magnetic field $B = .5\gamma$. The neutral gas which is injected from the orbiting spacecraft is expanding and moving with respect to the ionospheric plasma with the orbital velocity v_0 and is subject to collective ionization (CIV).

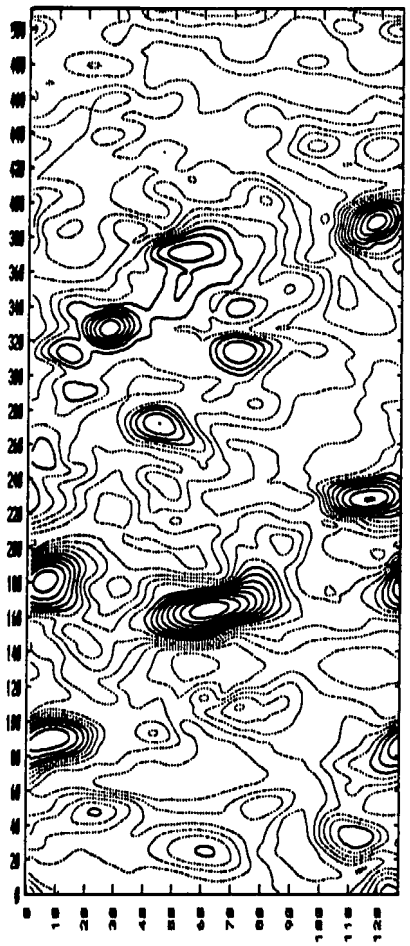

Figure 6: Contour map of the electrostatic potential over the simulation slab showing coherent structure that reflect the presence of strong plasma oscillations.

Figure (6) shows a planar contour map of the electrostatic potential over the plasma slab a few thousand plasma periods (about .2 msec) into the simulation. The coherent structure reflects the presence of strong plasma oscillations which are central to the electron energization process. The electron energization is illustrated in the associated plot of the electron distribution function shown in Fig. (7) where the formation of a suprathermal electron tail can be seen.

In terms of the parameters of the model in Section 2, the following numerical values can be extracted by fitting the model to the simulation results (after setting $\tau = 1$): $\mu \simeq .02$, $T_T \simeq .32\ eV$.

If we use the ratio $T_T/T_B = 3.2$ from the simulations to scale the tail of the distribution function for the low power thruster studied in Section 4, we would get $T_T = 6.4$. The λ_i values for $T_T = 6.4$ have been purposely plotted in Fig. (3) to illustrate this case. It can be seen from that figure that, for this value and for the tail fraction inferred from the simulation, we get a λ_i of a few millimeters.

6 Concluding Remarks

A prescription for the electron energy distribution function that allows the representation of suprathermal electron tails such as those produced by the nonlinear effects of plasma microturbulence has been combined with a detailed model of collisional excitation in argon. The resulting tool was used to investigate the effects of suprathermal tails on the minimum characteristic length for ionization. The ionization length which is at least 10 times smaller than that calculated assuming Maxwellian statistics is shown to be more consistent with distributions having suprathermal tail fractions and energies that could be produced by plasma microturbulence.

The numerical model can be easily extended to include other radiative-collisional processes. Ultimately, it can be used in fluid flow codes of the MPD thruster as an interface between the atomic physics and the nonlinear collective plasma processes.

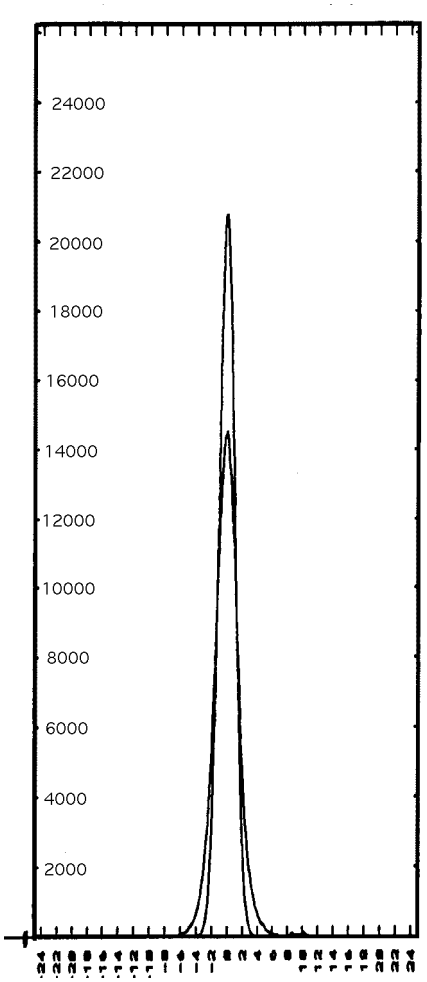

Figure 7: The velocity distribution functions $f(v_{ez})$, (where v_{ez} is the electron velocity along the magnetic field), at $t = t_0$ (large peak) and at a later time (small peak) showing the formation of the tail.

References

[1] A.P. Bruckner. *Spectroscopic Studies of the Exhaust Plume of a Quasi-Steady MPD Accelerator*. PhD thesis, Princeton University, Princeton, NJ, USA, 1972.

[2] E.Y. Choueiri, A.J. Kelly, and R.G. Jahn. The manifestation of Alfvén's hypothesis of critical ionization velocity in the performance of MPD thrusters. In 18^{th} *International Electric Propulsion Conference*, Alexandria, Virginia, USA, 1985. AIAA-85-2037.

[3] E.Y. Choueiri, A. J. Kelly, and R. G. Jahn. Current-driven instabilities of an electromagnetically accelerated plasma. In 20^{th} *International Electric Propulsion Conference*, Garmisch-Partenkirchen, W. Germany, 1988. AIAA-88-042.

[4] N. Brenning. Review of the CIV phenomenon. *Space Science Reviews*, 59:209–314, 1992.

[5] D.L. Tilley, E.Y. Choueiri, A.J. Kelly, and R.G. Jahn. An investigation of microinstabilities in a kW level self-field MPD thruster. In 22^{nd} *International Electric Propulsion Conference*, Viareggio, Italy, 1991. IEPC-91-122.

[6] H.P. Wagner, M. Auweter-Kurtz, and E. Messerschmid. Gradient influenced space charge instabilities in MPD thrusters. In 22^{nd} *International Electric Propulsion Conference*, Viareggio, Italy, 1991. IEPC-91-101.

[7] E.Y. Choueiri, A. J. Kelly, and R. G. Jahn. Current-driven plasma acceleration versus current-driven energy dissipation part II : Electromagnetic wave stability theory and experiments. In 22^{nd} *International Electric Propulsion Conference*, Viareggio, Italy, 1991. IEPC-91-100.

[8] V.A. Abramov, A.K. Vinogradova, Y.P. Dontsov, Y.A. Zavenyagin, P.E. Kovrov, V.I. Kogan, and A.I. Morozov. Investigation of electron temperature and plasma radiation in a quasi-stationary high-current discharge between coaxial electrodes. In *Proceedings of the Eighth International Conference on Phenomena in Ionized Gases*, 1968. Panel 33.1.11.

[9] T.M. Randolph, W.F. Von Jaskowsky, A. J. Kelly, and R. G. Jahn. Measurement of ionization levels in the interelectrode region of an MPD thruster. In 28^{th} *Joint Propulsion Conference*, Nashville, TN, 1992. AIAA-92-3460.

[10] R.K. Seals and H.A. Hassan. Analysis of MPD arcs with nonequilibrium ionization. *AIAA Journal*, 6(12):1452–1454, 1968.

[11] E.J. Sheppard and M. Martinez-Sanchez. Nonequilibrium ionization in MPD thrusters. In 21^{st} *International Electric Propulsion Conference*, Orlando, Florida, 1990. AIAA-90-2608.

[12] E.J. Sheppard and M. Martinez-Sanchez. Ionization ignition at the inlet of an MPD thruster. In 22^{nd} *International Electric Propulsion Conference*, Viareggio, Italy, 1991. IEPC-91-088.

[13] T.M. Randolph, 1993. Personal communication.

[14] H.W. Drawin. Collision and transport cross-sections. Technical Report EUR-CEA-FC-383, Euratom-CEA, 1967.

[15] J. Vlcek. A collisional-radiative model applicable to argon discharges over a wide range of conditions. *Journal of Physics D*, 22:623–631, 1989.

[16] W.W. Lee and H. Okuda. A simulation model for studying low frequency microinstabilities. *Journal of Computational Physics*, 26:139, 1978.

[17] J.A. Marshall, J.L. Burch, E.Y. Choueiri, and N. Kawashima. CIV experiments on ATLAS-1. *Geophysical Research Letters*, 20(6):499–502, 1993.